International Journal of Nanomedicine

Dovepress
open access to scientific and medical research

Open Access Full Text Article

ORIGINAL RESEARCH

A Rare-Earth Near-Infrared Nanoprobe for the Identification of Small Cell Lung Cancer

Liyun Xu[1], Lingling Fan[2], Jun Zhu[3]

[1]Department of Respiratory Medicine, Shanghai Pulmonary Hospital, Tongji University School of Medicine, Shanghai, 200433, People's Republic of China; [2]Department of Obstetrics and Gynecology, Obstetrics and Gynecology Hospital, Fudan University, Shanghai, 200011, People's Republic of China; [3]Department of Oncology, Shanghai Pulmonary Hospital, Tongji University School of Medicine, Shanghai, 200433, People's Republic of China

Correspondence: Jun Zhu, Department of Oncology, Shanghai Pulmonary Hospital, Tongji University School of Medicine, Shanghai, 200433, People's Republic of China, Email rotor121@sina.com; Lingling Fan, Department of Obstetrics and Gynecology, Obstetrics and Gynecology Hospital, Fudan University, Shanghai, 200011, People's Republic of China, Email fanlglg@hotmail.com

Background: Small cell lung cancer (SCLC) is a common subtype of lung cancer, and there is currently no established method for the early identification of SCLC. We prepared a novel rare-earth near-infrared (NIR) downconversion nanoprobe to identify SCLC cells.

Methods: The shell precursors Gd-OA and Na-TFA-OA were prepared, and the $NaYF_4$:Nd@$NaGdF_4$-ProGRP antibody probe was obtained after synthesizing downconversion fluorescent nanocrystals. The probe was used for NIR identification of cancer cells and subcutaneous tumors in nude mice. The biotoxicity of the probe to SCLC cells and nude mice was studied.

Results: The $NaYF_4$:Nd@$NaGdF_4$-ProGRP antibody probe was successfully prepared, with a size of 44 nm, an NIR emission peak at approximately 1060 nm, and a concentration of 40 μmol/mL. The probe could achieve accurate NIR identification of SCLC cells and subcutaneous tumors in nude mice. Optimal images of the subcutaneous tumor model were obtained approximately 10 minutes after probe injection. There was no significant change in the hematology indices, respiratory rate, or heart rate of nude mice after the probe was injected (all $P > 0.05$).

Conclusion: We have successfully prepared a low-toxicity probe that can identify SCLC cells, which may be useful for the early detection of SCLC. And conduct theoretical exploration for non-invasive identification and identification of some early metastatic lesions without pathological sampling in the future.

Keywords: probe, rare-earth, near-infrared, small cell lung cancer

Introduction

Lung cancer has the highest morbidity and mortality among all known cancer types. Its morbidity and mortality continue to increase, and lung cancer deaths accounted for 18% of all cancer-related deaths.[1] Small cell lung cancer (SCLC) is a common subtype of lung cancer, and there is currently a lack of probes for the early identification of SCLC.

Near-infrared fluorescence (NIRF) imaging has high sensitivity and high resolution for tumor detection, and rare-earth-doped downconversion nanomaterials are widely used in the biological field due to their advantages in NIRF imaging. The NIRF wavelength range is 700–1000nm. Current NIRF research has been extended to the second NIR window (NIR-II, 1000–1700nm), which further reduces tissue absorbance, autofluorescence and scattering, making NIR-II especially suitable for human applications.[2] The NIRF probe accumulates in solid tumors through blood circulation to the leakage site of blood vessels inside the tumor. The lysosomal proteases inside the tumor cells lysate to produce large molecules, releasing fluorescent pigments, which are detected by fluorescence imaging equipment,[3] with stronger penetration compared to quantum dots.[4] High levels of pro-gastrin-releasing peptide (ProGRP) are found in the serum of SCLC patients, which can be used as a marker of SCLC.[5] There are many antibodies that can recognize SCLC cells, but the ProGRP antibody has much higher specificity and sensitivity than neuron-specific enolase,[6] and the expression of ProGRP in non-SCLC is less than 4%.[7] The importance of the ProGRP antibody for the diagnosis of SCLC is recognized

Received: 20 July 2023
Accepted: 25 September 2023
Published: 2 October 2023

to be higher than that of neuron-specific enolase.[8] Therefore, in this experiment, the ProGRP antibody was selected as the probe to identify the specific target headgroup of SCLC.

This study constructed a rare-earth-doped NIR downconversion probe by using a rare-earth-doped downconversion nanomaterial and the ProGRP antibody (used as the target headgroup) to identify SCLC cells, it belonged to the near infrared nanoprobe.[9,10] Now the diagnosis of lung cancer is based on pathological testing after sampling the lung lesions, but early stage of lung cancer lesions are too small to obtain pathological diagnosis through sampling. The significance of this study is to construction probe, then create a non-invasive method for early identification of small cell lung cancer, thereby providing early medical intervention for the disease.

Materials and Methods

Probe Preparation

First, the shell precursor materials, the gadolinium-oleic acid (Gd-OA) precursor and the sodium-trifluoroacetic acid-oleic acid (Na-TFA-OA) precursor, were prepared. Then, neodymium (Nd)-doped downconversion fluorescent nanocrystals were synthesized. A ProGRP antibody was selected as the target headgroup on the surface of $NaYF_4$:Nd@$NaGdF_4$ to recognize cancer cells. By reaction with 1-ethyl-3-(3'-dimethylaminopropyl) carbodiimide-N-hydroxysuccinimide (EDC-NHS), the Pro-GRP antibody for cancer cell identification was linked to the downconversion nanocrystals. After the successful preparation of the probe, a performance characterization test of the probe was carried out. Finally, a $NaYF_4$:Nd@$NaGdF_4$-ProGRP antibody probe was prepared (Figure 1). The preparation and characterization process of the probe was complex and required many steps. For the specific preparation method, see Supplementary Materials.

Cytotoxicity Test of the Probe

In this experiment, the lung SCLC cell line HTB-119 was purchased from American Type Culture Collection (ATCC, Manassas, VA, USA). The cytotoxicity test process was as follows: 10 μL of the downconversion nanoprobe with different doping concentrations of rare earth elements was added to the cultured cell suspension and then 10 μL of Cell Counting Kit-8 (CCK-8, Abcam, UK) solution was added and incubated. Finally, the optical density (OD) of the cell suspensions with different concentrations of the probe was measured at 450 nm with a microplate reader to obtain the cytotoxicity of the probe to SCLC cells.

Cell Identification Imaging with the Probe

After the HTB-119 cells were incubated with 10 μL of the probe, the free nanocrystals were removed by centrifugation, and the centrifuged SCLC cell pellets were then placed in confocal dishes. The cells were identified with the probe under a NIRF microscope with a self-built platform equipped with a NIR vana charge-coupled device (NIRvana CCD, Princeton Instruments, USA) camera. The accuracy of cell identification imaging with the probe needed to be assessed.

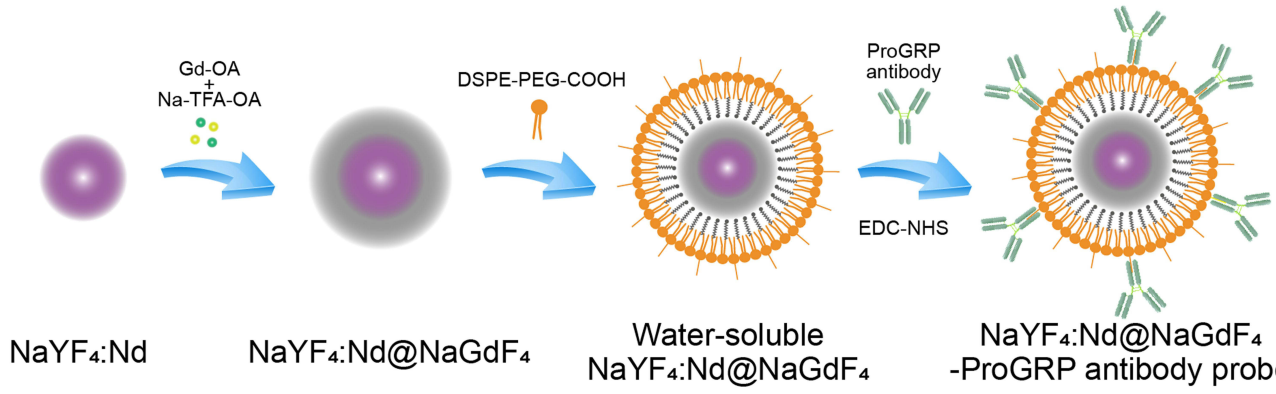

Figure 1 The process of preparing the nanoprobe.

4',6-diamidino-2-phenylindole (DAPI) is a fluorescent dye that can bind strongly to cellular deoxyribonucleic acid-(DNA), and DAPI staining is commonly used for fluorescence microscopy and is a standard method for cell identification. The accuracy of cell identification with the probe was determined by comparing the images of the cells identified with the probe with those of the cells identified with DAPI.

Identification of Subcutaneous SCLC Tumors in Nude Mice by the Probe

BALB/c nude mice (Shanghai Slake Experimental Animal Co., Ltd, China) were used for this experiment. All animal experimental procedures met the ethical requirements. After the SCLC HTB-119 cells were cultured, approximately 5×10^6 SCLC cells were subcutaneously injected into the right axilla of 5-week-old nude mice. The subcutaneous tumors were experimentally studied after reaching a diameter of 0.2–0.7 cm, which occurred approximately 12–28 days after the implantation of SCLC cells. After the successful growth of the subcutaneous tumors in the nude mice, they became tumor-bearing nude mice, and the subcutaneous tumors were confirmed by small-animal CT (Bruker Corporation, USA) imaging. The power of the built-in X-ray source was 25 W.

After the successful construction of the nude mouse subcutaneous tumor SCLC model, the prepared probe was used for NIR tracing. 200 μL of the probe was injected into the tail vein. After injection, the tumor-bearing nude mice were placed under the self-built NIRvana CCD camera platform for NIRF imaging, and the images were recorded after software processing. Moreover, the time after the probe was injected was recorded. NIRF imaging was performed at different times to determine when the optimal NIRF imaging effect could be obtained after probe injection. After NIR identification, the subcutaneous tumors and peritumoral tissue were excised and stained with hematoxylin-eosin (HE) to confirm whether the SCLC cells coincided with the tumors and whether there were tumor cells in the peritumoral tissue, thus determining whether the probe correctly identified the SCLC cells and their distribution range.

Toxicity of the Probe to Nude Mice with SCLC

Before probe injection, 100 μL venous blood was drawn from the tail vein of tumor-bearing nude mice for routine blood tests and liver and kidney function tests. Venous blood was drawn again from the tail vein of tumor-bearing nude mice after NIRF imaging with probe injection for routine blood tests and liver and kidney function tests. Next, after the nude mice were anesthetized, a mouse electrocardiogram (Shanghai Yuyan Scientific Instrument Co., Ltd, China) was used to observe the heart rate and respiratory rate of the nude mice before and after the probe was injected. Finally, routine blood test results, liver and kidney function analyses, and vital signs of the nude mice were analyzed before and after probe injection to clarify whether probe injection caused substantial changes in these parameters.

Experiment Ethics

This study was conducted at Shanghai Pulmonary Hospital, Tongji University School of Medicine, China. This study was approved by the Ethics Committee of Shanghai Pulmonary Hospital, Tongji University School of Medicine (Ethics approval No. K18-003-1) (the approval form also include the welfare of the laboratory animals). This study was carried out following the rules of the Declaration of Helsinki of 1975, revised in 2013.

Statistical Analysis

The values of hematology indices, respiratory rate, and heart rate of tumor-bearing nude mice were collected and analyzed by using SPSS software (International Business Machines Corporation, USA) for one-sample T tests.

Results

Probe Preparation

In this study, successive ion layer adsorption and reaction (SILAR)[11] was used to achieve uniform coating of the prepared probe nanocrystals around the core. The difficulty in synthesizing shell materials in the past was their own homogeneous nucleation.

After using SILAR, anions and cations were added in stages to avoid self nucleation. In the study, Na and Gd cations and F anions are added separately. However, the amount of anionic and cationic precursors added must be very accurate, especially in the later stage of multi-layer coating.[12,13] Then makes the surface smooth while reducing defects. Through the preliminary experimental steps of preparation, a water-soluble core-shell structured, efficient anti-quenching downconversion fluorescent nanocrystal, $NaYF_4$:Nd@$NaGdF_4$, was successfully prepared (Figure 2a). Transmission electron microscopy showed that the nanoparticles had a hexagonal shape. Finally, the $NaYF_4$:Nd@$NaGdF_4$-ProGRP antibody nanoprobe was obtained by hydration and surface modification of the nanocrystal with a ProGRP antibody as the target headgroup. The size of the probe prepared in this experiment was 44 nm (Figure 2b). Polymer dispersity index (PDI) of the probe was 0.607.

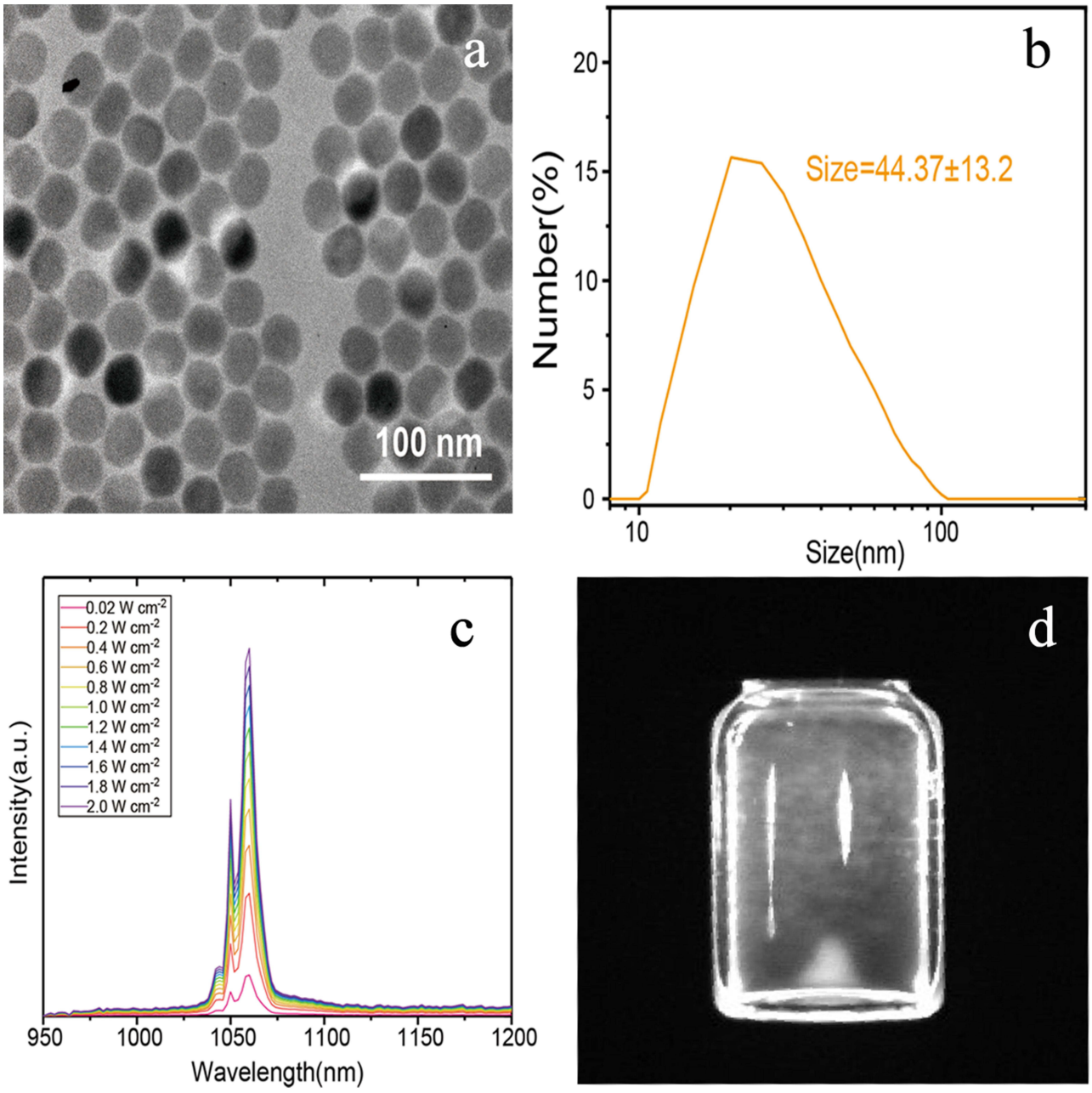

Figure 2 Characteristics of the $NaYF_4$:Nd@$NaGdF_4$-ProGRP antibody nanoprobe. (**a**) electron microscope image of $NaYF_4$:Nd@$NaGdF_4$ nanocrystals; (**b**) size of the $NaYF_4$:Nd@$NaGdF_4$-ProGRP antibody nanoprobe (44 nm); (**c**) emission spectrum of $NaYF_4$:Nd@$NaGdF_4$; (**d**) a near-infrared photograph of $NaYF_4$:Nd@$NaGdF_4$.

Emission Properties of the Probe

We tested the NIR and visible light spectra of the rare-earth-doped NIR downconversion nanoprobes. The probe was irradiated with a 980 nm NIR laser to obtain the emission spectra of $NaYF_4$:Nd@$NaGdF_4$ under different excitation powers (Figure 2c). The emission spectra of $NaYF_4$:Nd@$NaGdF_4$ showed an NIR emission peaks at approximately 1060 nm but no emission peak in the visible light region. The NIR emission of $NaYF_4$:Nd@$NaGdF_4$ is briefly shown in Figure 2d.

Cytotoxicity Testing and Imaging with the Probe

Under different concentration gradients of the $NaYF_4$:Nd@$NaGdF_4$-ProGRP antibody probe, the final survival rate of SCLC HTB-119 cells was above 60% after the cells were incubated with the probe for 4 hours, which indicated that $NaYF_4$:Nd@$NaGdF_4$-ProGRP antibody probe had low cytotoxicity to SCLC cells (Figure 3). Considering the proliferation toxicity of the probe to SCLC cells in the experiment and the reproducibility of the experiment, the final concentration of the probe was determined to be 40 μ mol/mL. After comparing the results of the identification imaging between the $NaYF_4$:Nd@$NaGdF_4$-ProGRP antibody probe and DAPI, it was revealed that the probe can accurately identify SCLC HTB-119 cells (Figure 4).

Construction of a Nude Mouse Subcutaneous SCLC Tumor Model

After subcutaneous injection of SCLC HTB-119 cells into BALB/c nude mice, the nude mouse subcutaneous SCLC tumor model was successfully constructed. After injection of SCLC cells, the mortality rate of nude mice was approximately 10%. Tumor-bearing nude mice were subjected to small-animal CT scans to find definitive evidence for the presence of subcutaneous tumors. The CT images showed that the subcutaneous injection of SCLC HTB-119 cells in BALB/c nude mice was successful (Figure 5).

NIR Tracking of Subcutaneous SCLC Tumors in Nude Mice

Before injection of the probe, no NIR signal was detected from the SCLC model mouse during NIRF imaging. After injection of the probe through the tail vein, NIR signals were detected from the subcutaneous tumors of the nude mice during NIRF imaging, and these signals were strongest approximately 10 minutes after probe injection (Figure 6). Therefore, NIR identification of subcutaneous tumors in the nude mouse subcutaneous SCLC tumor model was optimal 10 minutes after probe injection.

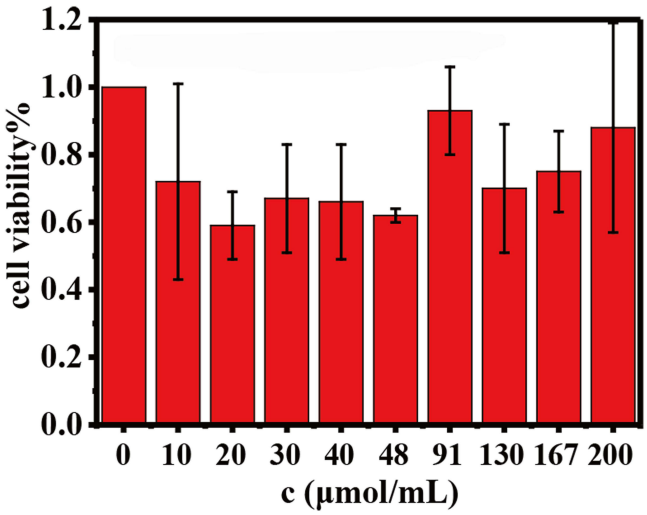

Figure 3 Toxicity of the NaYF4:Nd@NaGdF4-ProGRP antibody probe against HTB-119 cell proliferation (C, concentration of the probe).

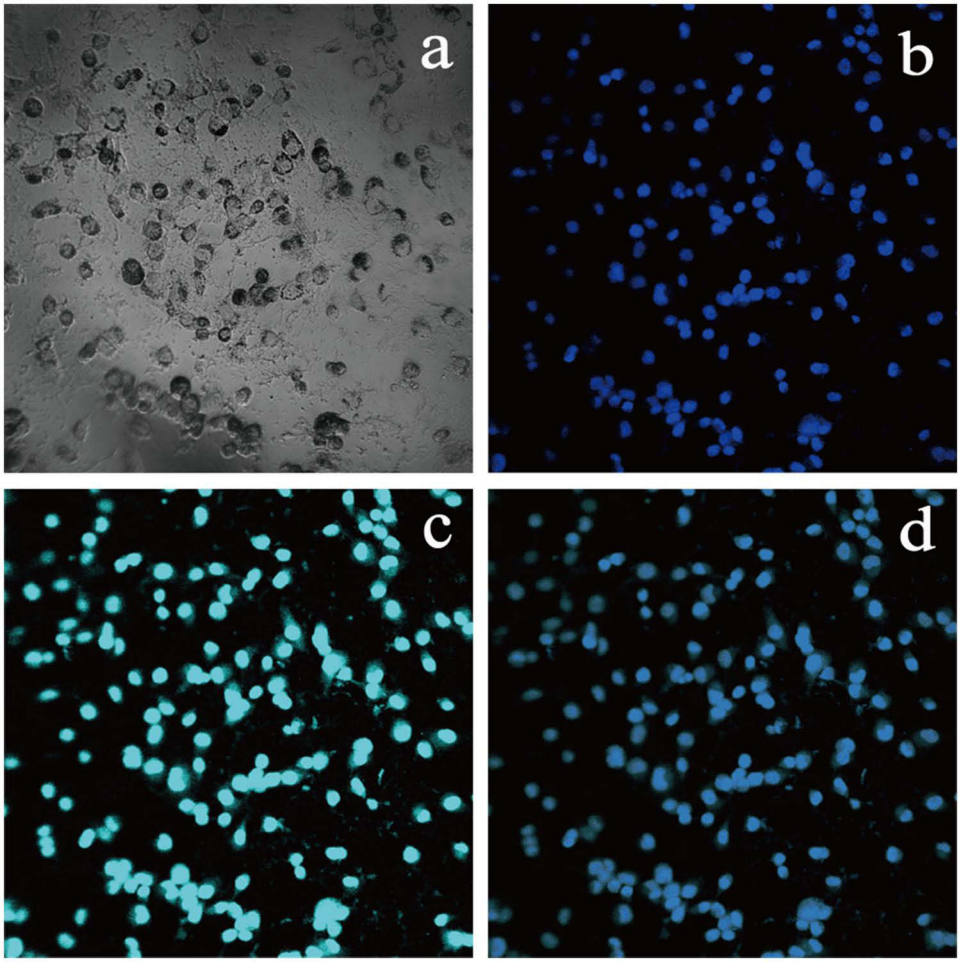

Figure 4 Near-infrared identification imaging with the probe. (**a**) micrograph of small-cell lung cancer HTB-119 cells; (**b**) DAPI imaging of small-cell lung cancer HTB-119 cells; (**c**) near-infrared identification imaging for HTB-119 cells with the $NaYF_4$:Nd@$NaGdF_4$-ProGRP antibody probe (cyan pseudocolor); (**d**) merged image of the HTB-119 cells identified by the $NaYF_4$:Nd@$NaGdF_4$-ProGRP antibody probe and those identified by DAPI imaging).

Accuracy of the Probe in Identifying Subcutaneous SCLC Tumors in Nude Mice

After NIR identification of the nude mouse subcutaneous tumor model with the probe, the subcutaneous tumors and peritumoral tissue were excised according to the guidance of fluorescence imaging, and the excised tumors and peritumoral tissue were subjected to HE staining. The subcutaneous tumor tissue cells were confirmed by pathological analysis to be SCLC cells (Figure 7). The probe identified the peritumoral tissue cells as normal tissue cells without cancer cell infiltration. The above results show that the probe accurately identified the SCLC cells and the distribution of SCLC cells and did not tag normal tissue cells.

Toxicity of the Probe to Nude Mice

100 μL of venous blood was drawn from the tail vein of nude mice with subcutaneous tumors before and 20 minutes and 60 minutes after tail vein injection of the probe into the mice. The blood samples were used for routine blood tests and liver and kidney function tests. The routine blood test results and liver and kidney function indices did not significantly change among these time points (all $P > 0.05$) (Table 1). The average heart rate of nude mice were 594±48 beats/min before probe injection, which was not significantly different from that (577±68 beats/min) 60 minutes after probe injection ($P > 0.05$). The respiratory rate before probe injection was 121±14 times/min, which was not significantly different from that (139±21 times/min) 60 minutes after probe injection ($P > 0.05$). Probe injection did not cause

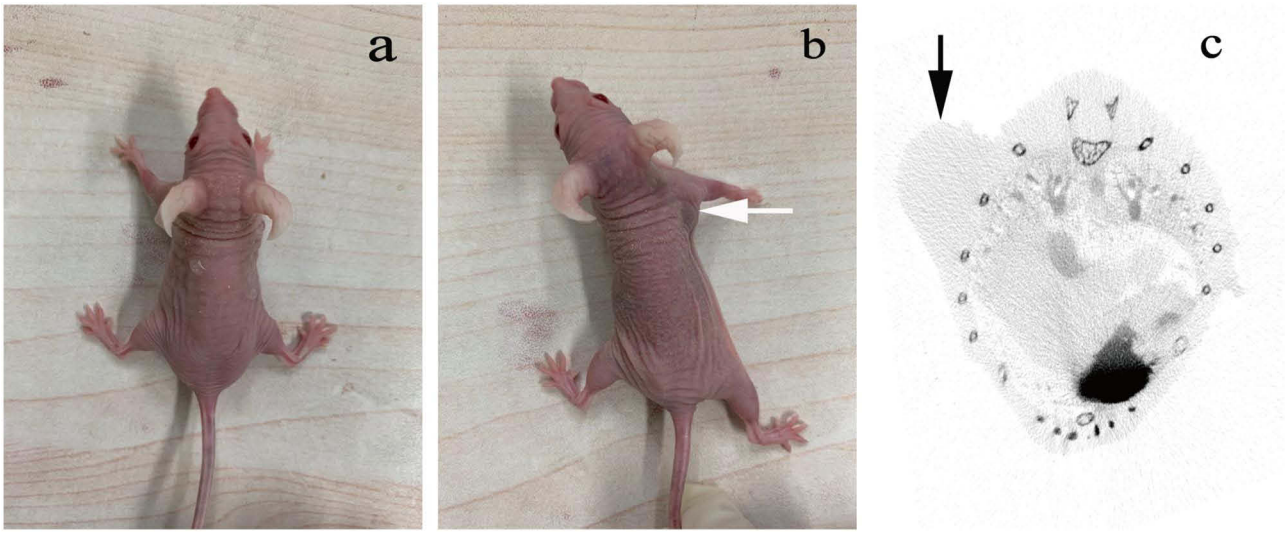

Figure 5 Nude mouse subcutaneous small-cell lung cancer tumor model. (**a**) BALB/c nude mouse; (**b**) a tumor-bearing nude mouse (the white arrow indicates the location of the subcutaneous tumor); (**c**) CT scan of the nude mouse lung cancer subcutaneous tumor model (the black arrow indicates the location of the subcutaneous tumor).

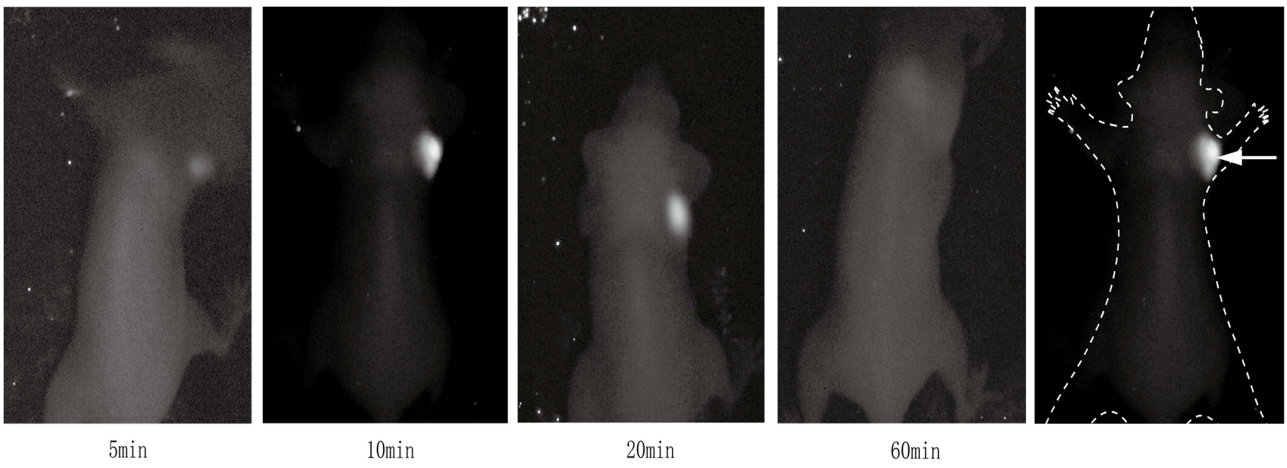

Figure 6 Near-infrared fluorescence images of the small-cell lung cancer HTB-119 subcutaneous tumor model in nude mice (the dashed line shows the best near-infrared fluorescence image, which was obtained 10 minutes after probe injection).

significant changes in the heart rate or respiratory rate of nude mice. These results show that the probe has low biotoxicity to the model mice.

Discussion

Biological tissues have low absorbance and autofluorescence in this wavelength range, so NIRF can achieve a deeper penetration depth in biological tissues with less background interference[14,15] and a higher signal-to-noise ratio.[16] Compared with conventional tomographic imaging techniques such as CT, PET-CT, and MRI, NIRF has the advantages of higher feedback speed, higher imaging resolution, higher sensitivity, lower cost, and no radiation. Therefore, NIRF has promising application potentials in the biological field. Rare-earth NIRF probes can achieve highly sensitive and noninvasive visualization of tumor cell distribution.[17] These characteristics are a foundation of selecting rare-earth downconversion materials as the probe shell in this experiment.

In this experiment, we prepared the $NaYF_4$:Nd@$NaGdF_4$-ProGRP antibody probe. The difficulty of probe preparation mainly lies in whether the rare-earth nanomaterial shell can be uniformly coated around the core. Probes fabricated by

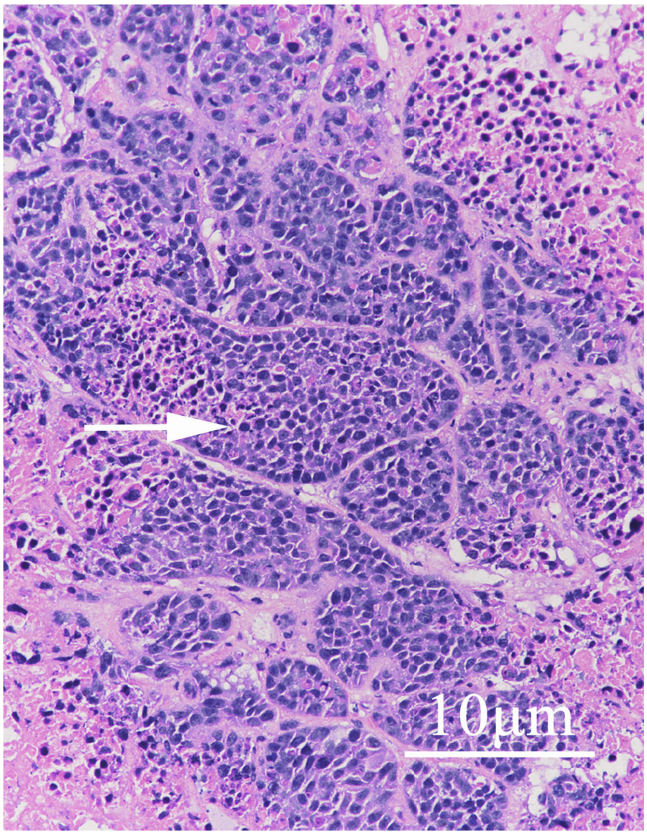

Figure 7 Image of HE-stained tissue area excised after identification of the subcutaneous small-cell lung cancer tumor in the nude mouse model with the probe (10 μm, the white arrow points to the cancer cells).

existing preparation methods often have obvious lattice defects within the rare-earth shell, poor passivation, and weak NIRF signals. In this experiment, we improved the preparation method. Specifically, we coated the probe core by using the SILAR method, which reduced the lattice defects of the shell nanocrystals. In addition, coating was divided into multiple monolayers to achieve orientated crystal growth, fewer crystal defects, and an organized arrangement. In this way, we achieved the optimal passivation effect and strong NIRF signals. The successfully prepared probe had an NIR emission peak of 1060 nm, which originates from the core-shell nanocrystalline Nd. Jiang's study showed that enhanced X-ray-excited afterglow imaging with an NIR-II emission peak at 1067 nm can be observed in Nd^{3+} dispersed in water,

Table 1 Hematology, Hepatotoxicity and Nephrotoxicity of the Probe to Small Cell Lung Cancer HTB-119 Subcutaneous Tumor Model Mice

Inspection Item		Before Injecting the Probe	20 Min After Injecting the Probe	60 Min After Injecting the Probe	P value
Blood routine	Hb (g/L)	168	166	171	0.840
	RBC ($\times 10^{12}$/L)	10.97	10.33	9.98	0.202
	WBC ($\times 10^{9}$/L)	6.52	6.07	7.23	0.821
	PLT ($\times 10^{9}$/L)	1281	1475	1236	0.568
Blood biochemistry	ALT (IU/L)	43.19	47.88	43.71	0.363
	AST (IU/L)	139	131	139	0.423
	TBIL (μmol/L)	2.49	2.49	2.59	0.423
	BUN (mmol/L)	6.36	6.60	6.24	0.742
	CREA (μmol/L)	35.74	32.61	34.22	0.228

human serum albumin solution, and a simulated lysosomal environment.[18] $NaGdF_4$:Nd 5%@$NaGdF_4$ had high sensitivity for liver cancer in NIR-II imaging and enhanced the MRI signal intensity difference between liver cancer tissue and peritumoral normal liver tissue.[19] Wu confirmed through experiments that NIR-II photons have a deeper optical penetration depth than NIR-I photons, which is based on the emission peak of Nd^{3+} at 1063 nm.[20] The emission peaks reported in the previous studies are all close to the distinct emission peak of this experiment.

The survival rate of SCLC cells after incubation with the $NaYF_4$:Nd@$NaGdF_4$-ProGRP antibody probe in the CCK test was greater than 60%. In the previous literature on rare-earth materials, Deka's Gd materials did not exhibit cytotoxic effects.[21] Zhang's $NaGdF_4$ nanoparticles were monodispersed in aqueous solution and had negligible cytotoxicity.[22] Deng's CaF2:Yb(3+)/Er(3+)/Mn(2+) hybrid microsphere structure had little cytotoxicity.[23] In view of the high histocompatibility and low cytotoxicity of rare-earth downconversion materials, the cytotoxicity of the probe prepared in this experiment was within the acceptable range. The concentration dose of the final probe selected for this study was 40μmol/mL, which was based on the research results of repeated experiments. When the probe was injected into the subcutaneous tumor model of nude mice, which concentration less than 40μmol/mL, there was no clear enhancement in the imaging of the probe within 5–20 minutes, and the boundary was relatively blurry. Between 50 to 80μmol/mL, the respiratory rate of the nude mouse model slightly increased. Greater than 90μmol/mL, based on CCK8 testing, the cell survival is unstable and the near-infrared signal is too strong. Based on the above comprehensive factors, we chose 40μmol/mL.

In the NIRF method to identify cells, DAPI, as a commonly used probe, can accurately stain the nuclei of cells.[24] DAPI can generally be used as a control method to evaluate the accuracy of new cell identification methods.[25] However, DAPI cannot be used for the identification of living cells in general because of its strong cytotoxicity,[26] which is the limiting factor for its application. The SCLC cells identified with the probe in this experiment were compared with those identified by the classical DAPI identification method, and the images of the two showed a high degree of overlap. Hence, the $NaYF_4$:Nd@$NaGdF_4$-ProGRP antibody probe could accurately identify SCLC cells.

In the nude mice subcutaneous SCLC tumor model experiment, the mortality rate of nude mice was approximately 10% after subcutaneous injection of SCLC cells. Several mice died directly after injection, which could have been caused by allergy or bleeding. Others died during tumor growth. Among these mice, some died due to the excessively large tumors as the they grew quickly, and others died after repeated convulsion likely due to high tumor malignancy or tumor metastases affecting the nervous system since the tumor growth rate was normal. However, the overall survival rate of the subcutaneous SCLC tumor model mice was approximately 90% at 3 weeks after inoculation. Before probe injection, NIRF imaging was performed on nude mice, and no NIRF signal was visualized. NIRF imaging was performed again after the probe was injected. Over time, the subcutaneous tumors were gradually visualized, and the tumor image was sharpest at a certain time point and then gradually faded until complete disappearance after approximately 90 minutes. The NIRF signal was the strongest at approximately 10 minutes after the probe was injected into nude mice, which indicated that the optimal imaging effect can be obtained 10 minutes after probe injection. After the probe was injected into nude mice, it could be quickly metabolized and cleared by kidneys. In Zheng's study, the renal clearance rate of NaGdF4 nanoparticles coated with polyacrylic acid was also excellent, with the remaining injection volume<3% 12 hours after injection.[27] Liang's experimental probe using Gd3+as a functionalized gold nanocluster could be quickly cleared from the body by kidneys.[28] Then, the tissue was excised along the areas displayed by NIRF imaging. Pathology confirmed that the lesions were composed of SCLC cells, with negative margins. Hence, the probe tracking in this experiment has high precision and accuracy.

Small cell lung cancer, as a pathological type with high malignancy and invasiveness in lung cancer, the gold standard for diagnosis is to obtain cytology or histology for pathological diagnosis.[29,30] Even in early stages of lung cancer, it is necessary to diagnose small cell lung cancer by obtaining a small quantity of cytological specimens, which can already been observed tumor lesions on CT or PET-CT. The advantage of this study is that cancer cells with a very small quantity of cells can be identified through probes, even if they are not demonstrated in imaging. To conduct theoretical exploration and research for non-invasive identification and identification of some early metastatic lesions without pathological sampling in the future.

In recent years, NIRF imaging has shown great potential in tumor research and has been applied in cell tissue imaging, in vivo imaging, tumor localization. However, few studies have applied NIRF imaging in lung cancer. Cohen used the lanthanide time-resolved fluorescence competitive binding assay to identify lung cancer cell lines with high and low endogenous δ expression, showing that NIRF has suitable selectivity for cancer cells.[31] Anti-epidermal growth factor receptor (anti-EGFR) nanoparticles coupled with an NIRF dye can robustly target EGFR.[32] In the well-studied in situ growth model of Lewis lung cancer cells in mice, NIRF probes can track tumor progression.[33] For some patients with resistance to targeted drugs, coupling NIRF photosensitizers to molecular targeted drugs can induce targeted drugs to enter tumor cells to generate strong fluorescence, and then targeted therapy can be combined with photodynamic therapy to overcome drug resistance.[34] However, NIRF imaging still has several technical limitations. For example, the spatial resolution of NIRF imaging is poor. Although NIRF imaging can display the focal point for in vivo imaging, it cannot perform accurate depth perception measurements.[35] Therefore, further technical improvements are needed.

Although some results had been obtained, the study still had certain limitations. Such as the selection of small cell lung cancer cell lines was relatively rare, multiple strains of cells could be selected for subsequent experiments to verify the accuracy of the probe. In addition, the cytotoxicity detection method only used CCK8 testing. Can other methods be added to verify the low toxicity of the probe again. These are the areas for further exploration in subsequent experiments. In the future, we hope to establish a situ cancer model of small cell lung cancer in nude mouse and validate the practicality of the probe. At the same time, we hope to establish a model of metastatic cancer and validate it with probe. Then gradually expand to other large animal models.

Conclusions

In this experiment, the $NaYF_4$:Nd@$NaGdF_4$-ProGRP antibody probe was successfully prepared, which can be used for accurate NIRF imaging identification of SCLC cells and subcutaneous tumor model mice with low biotoxicity. The probe provides a new method for the noninvasive identification of SCLC in the future.

Acknowledgments

We sincerely thank Fan Zhang and Lingfei Lu (Laboratory of Advanced Materials and Department of Chemistry, State Key Laboratory of Molecular Engineering of Polymers, Collaborative Innovation Center of Chemistry for Energy Materials, Fudan University, China), who provided basic theoretical and experimental technical support in this experiment.

Author Contributions

All authors made a significant contribution to the work reported, whether that was in the conception, study design, execution, acquisition of data, analysis and interpretation. All authors took part in drafting, revising the article. All authors gave final approval of the version to be published. All authors had agreed on the journal to which the article had been submitted. All authors agreed to be accountable for all aspects of the work.

Funding

This research received no specific grant from any funding agency in the public, commercial, or not-for-profit sectors.

Disclosure

The authors report no conflicts of interest regarding this article.

References

1. Houston KA, Mitchell KA, King J, White A, Ryan BM. Histologic Lung Cancer Incidence Rates and Trends vary by Race/Ethnicity and Residential County. *J Thorac Oncol*. 2018;13(4):497–509. doi:10.1016/j.jtho.2017.12.010
2. Miao Y, Gu C, Zhu Y, Yu B, Shen Y, Cong H. Recent Progress in Fluorescence Imaging of the Near-Infrared II Window. *Chembiochem*. 2018;19(24):2522–2541. doi:10.1002/cbic.201800466
3. Weissleder R, Tung CH, Mahmood U, Bogdanov A Jr. In vivo imaging of tumors with protease-activated near-infrared fluorescent probes. *Nat Biotechnol*. 1999;17(4):375–378. doi:10.1038/7933

4. Wang M, Abbineni G, Clevenger A, Mao C, Xu S. Upconversion nanoparticles: synthesis, surface modification and biological applications. *Nanomedicine*. 2011;7(6):710–729. doi:10.1016/j.nano.2011.02.013
5. Hassan A, Latif MT, Soo CI, et al. Short communication: diagnosis of lung cancer increases during the annual Southeast Asian haze periods. *Lung Cancer*. 2017;113:1–3. doi:10.1016/j.lungcan.2017.08.025
6. Dong A, Zhang J, Chen X, Ren X, Zhang X. Diagnostic value of ProGRP for small cell lung cancer in different stages. *J Thorac Dis*. 2019;11 (4):1182–1189. doi:10.21037/jtd.2019.04.29
7. Molina R, Filella X, Augé JM. ProGRP: a new biomarker for small cell lung cancer. *Clin Biochem*. 2004;37(7):505–511. doi:10.1016/j.clinbiochem.2004.05.007
8. Wojcik E, Kulpa JK. Pro-gastrin-releasing peptide (ProGRP) as a biomarker in small-cell lung cancer diagnosis, monitoring and evaluation of treatment response. *Lung Cancer*. 2017;8:231–240. doi:10.2147/LCTT.S149516
9. Zhou S, Jiang L, Li C, et al. Acid and Hypoxia Tandem-Activatable Deep Near-Infrared Nanoprobe for Two-Step Signal Amplification and Early Detection of Cancer. *Adv Mater*. 2023;35(36):e2212231. doi:10.1002/adma.202212231
10. Asha Krishnan M, Yadav K, Roach P, Chelvam V. A targeted near-infrared nanoprobe for deep-tissue penetration and imaging of prostate cancer. *Biomater Sci*. 2021;9(6):2295–2312. doi:10.1039/d0bm01970d
11. Zhang F, Che R, Li X, et al. Direct imaging the upconversion nanocrystal core/shell structure at the subnanometer level: shell thickness dependence in upconverting optical properties. *Nano Lett*. 2012;12(6):2852–2858. doi:10.1021/nl300421n
12. Li JJ, Wang YA, Guo W, et al. Large-scale synthesis of nearly monodisperse CdSe/CdS core/shell nanocrystals using air-stable reagents via successive ion layer adsorption and reaction. *J Am Chem Soc*. 2003;125(41):12567–12575. doi:10.1021/ja0363563
13. Joo J, Kim D, Yun DJ, et al. The fabrication of highly uniform ZnO/CdS core/shell structures using a spin-coating-based successive ion layer adsorption and reaction method. *Nanotechnology*. 2010;21(32):325604. doi:10.1088/0957-4484/21/32/325604
14. Hilderbrand SA, Weissleder R. Near-infrared fluorescence: application to in vivo molecular imaging. *Curr Opin Chem Biol*. 2010;14(1):71–79. doi:10.1016/j.cbpa.2009.09.029
15. Yang X, Shi C, Tong R, et al. Near IR heptamethine cyanine dye-mediated cancer imaging. *Clin Cancer Res*. 2010;16(10):2833–2844. doi:10.1158/1078-0432.CCR-10-0059
16. Amiot CL, Xu S, Liang S, Pan L, Zhao JX. Near-Infrared Fluorescent Materials for Sensing of Biological Targets. *Sensors*. 2008;8(5):3082–3105. doi:10.3390/s8053082
17. Mei X, Ma J, Bai X, et al. A bottom-up synthesis of rare-earth-hydrotalcite monolayer nanosheets toward multimode imaging and synergetic therapy. *Chem Sci*. 2018;9(25):5630–5639. doi:10.1039/c8sc01288a
18. Jiang R, Yang J, Meng Y, et al. X-ray/red-light excited ZGGO:Cr, Nd nanoprobes for NIR-I/II afterglow imaging. *Dalton Trans*. 2020;49 (18):6074–6083. doi:10.1039/d0dt00247j
19. Ren Y, He S, Huttad L, et al. An NIR-II/MR dual modal nanoprobe for liver cancer imaging. *Nanoscale*. 2020;12(21):11510–11517. doi:10.1039/d0nr00075b
20. Wu L, Hu J, Zou Q, et al. Synthesis and optical properties of a Y 3(Al/Ga) 5 O 12:Ce 3+, Cr 3+, Nd 3+ persistent luminescence nanophosphor: a promising near-infrared-II nanoprobe for biological applications. *Nanoscale*. 2020;12(26):14180–14187. doi:10.1039/d0nr03269g
21. Deka S, Saxena V, Hasan A, Chandra P, Pandey LM. Synthesis, characterization and in vitro analysis of α-Fe 2 O 3-GdFeO 3 biphasic materials as therapeutic agent for magnetic hyperthermia applications. *Mater Sci Eng C Mater Biol Appl*. 2018;92:932–941. doi:10.1016/j.msec.2018.07.042
22. Zhang W, Zhang S, Gao P, et al. The feasibility of NaGdF 4 nanoparticles as an x-ray fluorescence computed tomography imaging probe for the liver and lungs. *Med Phys*. 2020;47(2):662–671. doi:10.1002/mp.13930
23. Deng X, Dai Y, Liu J, et al. Multifunctional hollow CaF2:Yb(3+)/Er(3+)/Mn(2+)-poly(2-Aminoethyl methacrylate) microspheres for Pt(IV) pro-drug delivery and tri-modal imaging. *Biomaterials*. 2015;50:154–163. doi:10.1016/j.biomaterials.2015.01.040
24. Kapuscinski J. DAPI: a DNA-specific fluorescent probe. *Biotech Histochem*. 1995;70(5):220–233. doi:10.3109/10520299509108199
25. Buzin AR, Pinto FE, Nieschke K, et al. Replacement of specific markers for apoptosis and necrosis by nuclear morphology for affordable cytometry. *J Immunol Methods*. 2015;420:24–30. doi:10.1016/j.jim.2015.03.011
26. Borowy NK, Fink E, Hirumi H. In vitro activity of the trypanocidal diamidine DAPI on animal-infective Trypanosoma brucei brucei. *Acta Trop*. 1985;42(4):287–298.
27. Zheng XY, Zhao K, Tang J, et al. Gd-Dots with Strong Ligand-Water Interaction for Ultrasensitive Magnetic Resonance Renography. *ACS Nano*. 2017;11(4):3642–3650. doi:10.1021/acsnano.6b07959
28. Liang G, Xiao L. Gd 3+-Functionalized gold nanoclusters for fluorescence-magnetic resonance bimodal imaging. *Biomater Sci*. 2017;5 (10):2122–2130. doi:10.1039/c7bm00608j
29. Hoschek S, Hoschek-Risslegger U, Fiegl M, et al. Small cell lung cancer. *Wien Klin Wochenschr*. 2007;119(23–24):697–710. doi:10.1007/s00508-007-0913-1
30. Serke M, Schönfeld N. Diagnosis and staging of lung cancer. *Dtsch Med Wochenschr*. 2007;132(21):1165–1169. doi:10.1055/s-2007-979393
31. Cohen AS, Patek R, Enkemann SA, et al. Delta-Opioid Receptor (δOR) Targeted Near-Infrared Fluorescent Agent for Imaging of Lung Cancer: Synthesis and Evaluation In Vitro and In Vivo. *Bioconjug Chem*. 2016;27(2):427–438. doi:10.1021/acs.bioconjchem.5b00516
32. Wan J, Wu W, Zhang R, Liu S, Huang Y. Anti-EGFR antibody conjugated silica nanoparticles as probes for lung cancer detection. *Exp Ther Med*. 2017;14(4):3407–3412. doi:10.3892/etm.2017.4988
33. Ma X, Phi Van V, Kimm MA, et al. Integrin-Targeted Hybrid Fluorescence Molecular Tomography/X-ray Computed Tomography for Imaging Tumor Progression and Early Response in Non-Small Cell Lung Cancer. *Neoplasia*. 2017;19(1):8–16. doi:10.1016/j.neo.2016.11.009
34. Gao Y, Zhang H, Zhang Y, et al. Erlotinib-Guided Self-Assembled Trifunctional Click Nanotheranostics for Distinguishing Druggable Mutations and Synergistic Therapy of Nonsmall Cell Lung Cancer. *Mol Pharm*. 2018;15(11):5146–5161. doi:10.1021/acs.molpharmaceut.8b00561
35. Lee S, George Thomas R, Ju Moon M, et al. Near-Infrared Heptamethine Cyanine Based Iron Oxide Nanoparticles for Tumor Targeted Multimodal Imaging and Photothermal Therapy. *Sci Rep*. 2017;7(1):2108. doi:10.1038/s41598-017-01108-5